Metabolite Production in Patients with Lymphoma After Radiometal-Labeled Antibody Administration

Gerald L. DeNardo, Sally J. DeNardo, David L. Kukis, Robert T. O'Donnell, Sui Shen, Gary R. Mirick, and Claude F. Meares

Department of Internal Medicine, University of California Davis Medical Center, Sacramento; and Department of Chemistry, University of California Davis, Davis, California

Radiometal-labeled monoclonal antibodies are retained longer in tumors than iodinated antibodies, leading to their increased use for radioimmunotherapy. Dissociation of radioiodine from the antibody during metabolism has been documented. We now report metabolites in the plasma of lymphoma patients given ^{111}In- and ^{90}Y-2-iminothiolane-2-[*p*-(bromoacetamido)benzyl]-1,4,7,10-tetraazacyclododecane-*N*,*N*′,*N*″,*N*‴-tetraacetic acid-Lym-1 (^{111}In/^{90}Y-2IT-BAD-Lym-1). **Methods:** Nineteen patients with non-Hodgkin's lymphoma (NHL) received ^{111}In- and ^{90}Y-2IT-BAD-Lym-1; ^{111}In was used as a surrogate tracer for ^{90}Y, which emits no γ-photon. Plasma was obtained up to 7 d and analyzed by high-performance liquid chromatography to determine the fraction of radiolabel associated with monomeric antibody, metabolites, and complexed antibody. Planar images of conjugate views were acquired up to 7 d and used to quantitate ^{111}In in organs and tumors. **Results:** Metabolites and complexes were observed in the plasma of every patient who received ^{111}In-2IT-BAD-Lym-1. At 3 d, the mean percentages of ^{111}In in the patients' plasma in monomeric, metabolite, and complexed forms were 54%, 36%, and 10%, respectively. Metabolites of ^{90}Y-2IT-BAD-Lym-1 were formed to a similar extent. In comparison, in groups of breast and prostate cancer patients who received the radioimmunoconjugate ^{111}In-2IT-BAD-m170, 91% and 94% of ^{111}In in the patients' plasma were in monomeric form, respectively. Metabolites and complexes of ^{111}In-2IT-BAD-Lym-1 contributed a mean 10% of the total area under the time–activity curve (AUC) for blood. Little formation of metabolites and complexes occurred in vitro in NHL patient or volunteer plasma or in Raji cell culture. The clinical and in vitro data supported the processing of ^{111}In/^{90}Y-2IT-BAD-Lym-1 in the hepatocytes as the dominant mechanism for the production of metabolites. **Conclusion:** Metabolites of ^{111}In/^{90}Y-2IT-BAD-Lym-1 accounted for 10% of blood AUC in patients. The therapeutic index was adversely affected by metabolism of ^{111}In/^{90}Y-2IT-BAD-Lym-1 to the extent that the tumor specificity of the radioactive metabolites was lost.

Key Words: antibodies; antibody conjugates; cancer; lymphoma; Lym-1; metabolism; radioimmunotherapy

J Nucl Med 2001; 42:1324–1333

Received Nov. 17, 2000; revision accepted May 2, 2001.

For correspondence or reprints contact: Gerald L. DeNardo, MD, Molecular Cancer Institute, 1508 Alhambra Blvd., Suite 3100, Sacramento, CA 95816.

The area under the curve (AUC) for the blood concentrations of a drug is commonly used to characterize its pharmacokinetic behavior in patients. In the case of radioimmunotherapy using a monoclonal antibody (mAb) labeled with a radionuclide tracer under appropriate conditions, the AUC can be determined by counting sequential blood samples. To the extent that the radionuclide tracks the antibody, the pharmacokinetics of the radiolabeled antibody can be determined for all tissues of the body in a noninvasive manner using quantitative scintigraphy, a remarkable asset. Typically, the stability of the radiolabeled antibody over time in a biologic milieu, such as serum or plasma, is established in preclinical studies (*1,2*). However, for radioiodinated antibodies the radiolabel is dissociated from the antibody during metabolism (*3–6*). In such instances, the pharmacokinetic behavior reflects, in part, that of the radionuclide rather than that of the antibody. In any event, the resulting dosimetric determinations are accurate because it is the pharmacokinetics of the radionuclide that determines radiation dose distribution.

Lym-1 has had little therapeutic effectiveness in non-Hodgkin's lymphoma (NHL) when used for immunotherapy (*7*), but it has proven highly effective for NHL and B-cell chronic lymphocytic leukemia when used to target radionuclides to malignant tissue (*8,9*). All histologic grades of chemotherapy-resistant NHL were responsive to ^{131}I-Lym-1 or ^{67}Cu-2-iminothiolane-6-[*p*-(bromoacetamido)benzyl]-1,4,7,11-tetraazacyclotetradecane-*N*,*N*′,*N*″,*N*‴-tetraacetic acid-Lym-1 (^{67}Cu-2IT-BAT-Lym-1) (*10,11*). Radiometals, delivered by antibody carrier molecules, are retained in tumors longer than ^{131}I (albeit also in normal tissues, particularly liver), leading to their increased use for radioimmunotherapy. ^{90}Y was attractive for radioimmunotherapy because it emits abundant, highly energetic β-emissions that deliver a higher radiation dose per unit of radioactivity than ^{131}I or ^{67}Cu (*12*) and is commercially available. We have used the anti-mouse lymphoma IgG2a Lym-1, radiolabeled as ^{90}Y-2-iminothiolane-2-[*p*-(bromoacetamido)benzyl]-1,4,7,10-tetraazacyclododecane-*N*,*N*′,*N*″,*N*‴-tetraacetic acid-

Lym-1 (^{90}Y-2IT-BAD-Lym-1), for therapy of NHL (*13*). ^{111}In was used as a surrogate tracer for ^{90}Y, which lacks a γ-photon emission. 1,4,7,10-Tetraazacyclododecane-*N*,*N*′,*N*″,*N*‴-tetraacetic acid (DOTA) was designed specifically to bind ^{90}Y tightly, and ^{90}Y- and ^{111}In-2IT-BAD-Lym-1 radioimmunoconjugates (RICs) of high purity, exceptional stability, and complete retention of functional and structural integrity are routinely produced (*1*,*13*,*14*). Molecular sieving high-performance liquid chromatography (HPLC) of plasma and urine samples in phase I trials has been used to confirm that the radionuclide in the plasma remained attached to a species having a molecular weight (MW) corresponding to an mAb, and not lower (metabolites) or higher (complexes) MWs (*15*,*16*). HPLC thus served as a simple surrogate for assays of immunoreactivity.

Soon after injection of ^{111}In- or ^{90}Y-2IT-BAD-Lym-1, radiolabeled metabolites and complexes were observed in the plasma of every patient by routine HPLC evaluation. Metabolites of iodinated mAbs, including Lym-1, are routinely identified in patient urine, and to a much lesser extent in the stool (*8*), but do not commonly accumulate in the plasma. Similarly, metabolites of radiometal-labeled mAbs have been reported in urine of patients (*17*) but not, to our knowledge, in plasma. In this study, the nature of the metabolites, their impact on therapeutic indices (TIs), and the mechanisms of formation were investigated. The results were compared with those for an antiadenocarcinoma antibody labeled in an analogous fashion and given to patients with breast or prostate cancer.

MATERIALS AND METHODS

Patient Population

Nineteen patients with B-lymphocyte NHL that had progressed despite standard therapy entered studies of ^{111}In-2IT-BAD-Lym-1. The mean age was 53 y (range, 33–77 y). NHL was classified according to the Working Formulation (*18*), and all grades of lymphoma were eligible for study entry. The mean Karnofsky performance status was 82 (range, 60–90). Lym-1 reactivity was shown in all patients by immunohistologic staining or positive tumor imaging. Two patients had prior splenectomies.

The plasma of all 19 patients who received ^{111}In-2IT-BAD-Lym-1 was examined by radioanalytic HPLC, as described below, for metabolites and complexes. The plasma of 3 of these patients, who subsequently received ^{90}Y-2IT-BAD-Lym-1, was examined by radioanalytic HPLC. Thus, plasma HPLC data were obtained from a "parent group" of 19 patients receiving ^{111}In-2IT-BAD-Lym-1 and a subgroup of 3 patients providing comparative data for ^{111}In- and ^{90}Y-2IT-BAD-Lym-1.

Patients with metastatic prostate cancer (n = 15) that had become refractory to hormonal therapy entered studies of ^{111}In- and ^{90}Y-2IT-BAD-m170. The mean age was 64 y (range, 54–76 y). The mean Karnofsky performance status was 85 (range, 70–90). m170 reactivity was shown in all patients by positive tumor imaging.

Patients with breast cancer (n = 7) that had progressed despite standard therapy entered studies of ^{111}In- and ^{90}Y-2IT-BAD-m170. The mean age was 45 y (range, 41–50 y). The mean Karnofsky performance status was 81 (range, 70–90). m170 reactivity was shown in all patients by immunohistochemical staining or positive tumor imaging.

Patients were eligible if their serum tested negative for human antimouse antibody (HAMA), they had received no other cancer therapy for at least 4 wk, they had measurable disease at the time of entry, and they met additional trial-specific criteria. Before trial entry, patients signed an informed consent that was approved by the University of California at Davis human subjects and radiation use committees under an investigational new drug authorization from the U.S. Food and Drug Administration.

Antibodies

Lym-1 (Damon Biotechnology, Needham Heights, MA; or Techniclone, Inc., Tustin, CA) is a nonshedding, noninternalizing IgG2a mouse mAb with high affinity for a discontinuous epitope on the β-subunit of human leukocyte antigen (HLA)-DR10, located on the surface membrane of malignant B-lymphocytes (*19*). m170 (Biomira, Inc., Edmonton, Alberta, Canada) is an IgG1 mouse mAb used in clinical trials for therapy of breast cancer and other adenocarcinomas (*20*). Biopsy specimens of metastatic breast cancer revealed that 90% of tumors were stained abundantly with m170 (*21*).

Radiolabeling

2IT-BAD-Lym-1 and 2IT-BAD-m170 were conjugated and radiolabeled with ^{111}In (Mallinckrodt, St. Louis, MO; Amersham, Arlington Heights, IL; or Nordion, Kanata, Ontario, Canada) or ^{90}Y (Pacific Northwest National Laboratory, Richland, WA) as described (*13*,*14*). ^{111}In-2IT-BAD-Lym-1, ^{90}Y-2IT-BAD-Lym-1, and ^{111}In-2IT-BAD-m170 were purified and transferred to sterile saline by gel filtration chromatography. Patient doses were filtered (0.22 μm) and formulated at 37 MBq/mL in 4% human serum albumin/saline.

Lym-1 and m170 were radiolabeled with ^{125}I (ICN Radiochemicals, Irvine, CA) as reference standards for radioimmunoassays. ^{125}I-Lym-1 was prepared by the chloramine-T reaction (Sigma Chemical, St. Louis, MO) to a final specific activity of 40 MBq/mg Lym-1. ^{125}I-m170 was prepared with IODO-GEN iodination reagent (Pierce, Rockford, IL) at 350 MBq/mg m170. The specific activities were chosen to provide sufficient counts for the assays.

Quality Assurance

Radiopharmaceuticals were evaluated before injection for structural and functional integrity by HPLC, cellulose acetate electrophoresis (CAE), and radioimmunoassay, except the radioimmunoassay of ^{111}In-2IT-BAD-m170 was performed retrospectively on decayed samples. HPLC of radiopharmaceuticals (Beckman, Fullerton, CA) was performed using a gel filtration column (BiosepSEC 3000; Phenomenex, Torrance, CA [or equivalent]) eluted in 0.1 mol/L sodium phosphate buffer, pH 7, at a flow rate of 1.0 mL/min. HPLC traces were monitored by ultraviolet absorbance (280 nm) and radioanalytic detection.

CAE (Gelman Sciences, Inc., Ann Arbor, MI) was performed using 0.05 mol/L sodium barbital buffer, pH 8.6. A current of 5 mA per strip was applied. Samples were electrophoresed for 11 min to resolve small species (i.e., free radiochelates) from immunoconjugates and 45 min to resolve high MW species (e.g., immunoconjugate aggregates) from monomers. Detection and quantitation were by radiation scanning (AMBIS, San Diego, CA).

The immunoreactivity of ^{111}In- and ^{90}Y-2IT-BAD-Lym-1 was assessed by solid-phase radioimmunoassay against partially purified membrane fragments from Raji cells as described (*22*). The immunoreactivity of ^{111}In-2IT-BAD-m170 was assessed by a competitive assay against rabbit anti-m170 idiotype antibody. The rabbit anti-m170 idiotype antibody binds m170 near the m170-antigen binding site; thus, its ability to bind m170 indicates that the m170-antigen binding site is intact. Decayed ^{111}In-2IT-BAD-m170 (0, 1.25, 2.5, 5.0, 10, 20, or 40 ng) and ^{125}I-m170 (4 ng) were incubated in a test tube coated with rabbit anti-m170 idiotype antibody for 2 h at room temperature. The fraction of ^{125}I-m170 bound in the absence of ^{111}In-2IT-BAD-m170 was the maximum binding fraction. The amount of decayed ^{111}In-2IT-BAD-m170 required to reduce ^{125}I-m170 binding to half of the maximum binding fraction (ED_{50}) was determined. Thus, a smaller ED_{50} indicated higher immunoreactivity. A parallel study was performed, in which the ED_{50} of the m170 reference standard was assessed. The relative immunoreactivity of ^{111}In-2IT-BAD-m170 was calculated as the quotient, ED_{50} reference standard/ED_{50} ^{111}In-2IT-BAD-m170.

Antibody Injection

Unmodified Lym-1 or m170 was given before radiolabeled Lym-1 or m170, respectively, to block nonspecific binding sites and provide stable pharmacokinetics (*23*). The total unmodified plus radiolabeled antibody injected, at a rate of 0.5–1.0 mg/min, was 6.3–31 mg in patients receiving ^{111}In-2IT-BAD-Lym-1 and 5.1–11 mg in patients receiving ^{111}In-2IT-BAD-m170, depending on the specific activity of the radiopharmaceutical.

Analysis of Blood and Urine

Blood samples were obtained immediately, during the next 6 h, and daily up to 7 d after injection of radiopharmaceuticals. Blood was collected in Vacutainer test tubes that were coated with buffered sodium citrate to prevent clotting (Becton Dickinson, Franklin Lakes, NJ). Blood samples (0.1 or 0.5 mL) were counted to obtain the concentration of ^{111}In or ^{90}Y in the blood. The remainder of the blood was centrifuged, the plasma was decanted, and fresh plasma samples (0.1 mL) were examined by HPLC, as described, on the day received. HPLC eluant fractions (0.5 mL) were collected (Gilson, Inc., Middleton, WI), and their activities were measured in a γ-well counter (Pharmacia Biotech, Inc., Piscataway, NJ). HPLC traces of unmodified Lym-1 and m170 indicated an elution time of 9.9 ± 0.2 min (i.e., apparent MW, 147 ± 25 kilodaltons [kDa]) based on a standard curve using MW standard proteins (Bio-Rad, Hercules, CA). The correspondence between elution volume and MW according to the standard curve is shown in Figure 1. To allow for variability in HPLC performance, individual radioanalytic HPLC traces and fraction counts were evaluated to designate peaks as complexes, monomers, and metabolites. Generally, HPLC fractions collected over the range 7–9 mL, 9–12 mL, and 12–18 mL were designated as complexes, monomers, and metabolites, respectively.

Immunoprecipitation studies were performed to further characterize the radioactive species in plasma, specifically, to test for the transchelation of radiometals to serum proteins. Affinity-purified antialbumin and antitransferrin antibodies (Sigma) were added to plasma from an NHL patient receiving ^{111}In-2IT-BAD-Lym-1, and from an NHL patient receiving ^{90}Y-2IT-BAD-Lym-1, and precipitated as described (*16*).

Urine was collected up to 7 d after infusion of radiopharmaceuticals. Aliquots of urine (0.1 mL) were assayed in a γ-well counter and then multiplied by the measured urine volume to calculate output of ^{111}In or ^{90}Y.

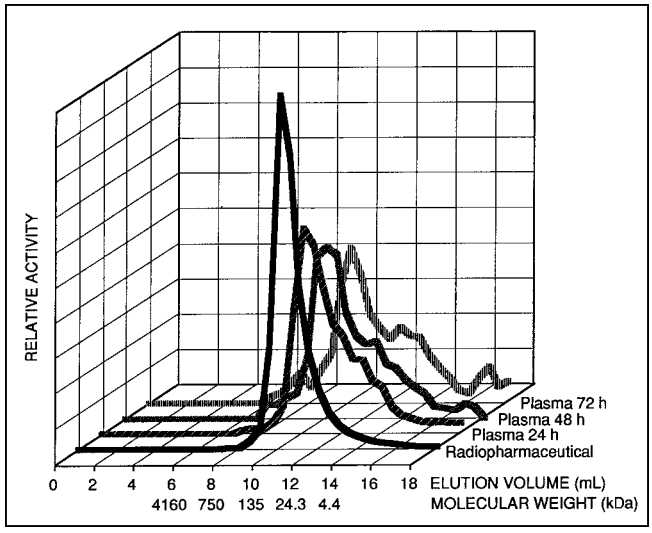

FIGURE 1. Radioanalytic HPLC traces of ^{111}In-2IT-BAD-Lym-1 radiopharmaceutical before injection in NHL patient (front trace) and of patient plasma 24, 48, and 72 h after injection. Percentage of ^{111}In in patient's plasma associated with metabolites (elution volume, 12–18 mL) and complexes (elution volume, 7–9 mL) increased over time. Similar pattern was observed for every NHL patient who received ^{111}In-2IT-BAD-Lym-1. Standard curve from MW standard proteins was used to relate elution volume to MW.

Pharmacokinetics

The cumulated activity of ^{111}In in the blood was obtained by fitting the percentage injected dose (%ID) of ^{111}In in the blood versus time to a biexponential function (*13*). The cumulated activity in the blood from monomeric ^{111}In-2IT-BAD-Lym-1 was also calculated as follows. At each time point, the %ID of ^{111}In in the blood was multiplied by the fraction of ^{111}In as monomeric ^{111}In-2IT-BAD-Lym-1 from HPLC analysis of plasma. These data, %ID of ^{111}In as monomeric ^{111}In-2IT-BAD-Lym-1 versus time, were fitted to a biexponential function. The cumulated activities of ^{90}Y in the blood, from all species and from monomeric ^{90}Y-2IT-BAD-Lym-1, were calculated by similar methods.

Methods for obtaining pharmacokinetic data for ^{111}In-2IT-BAD-Lym-1 and ^{111}In-2IT-BAD-m170 in organs and tumors have been described (*24*). Briefly, planar images of conjugate views were acquired immediately, during the next 6 h, and daily for 3–7 d after injection of radiopharmaceuticals and used to quantitate ^{111}In in organs and tumors.

The cumulated activity in tissues was determined by integrating the time–activity curve over time. Pharmacokinetic data in tissues were usually fit to a monoexponential function to calculate cumulated activity. However, in some instances, the uptake in tumor or liver increased continuously over the imaging period of a week; in these instances, the cumulated activities were determined by fitting the data to a cubic spline function up to the last imaging data point and then assuming a constant concentration afterward. Except for the spleen, MIRD reference man masses were used for all organs to obtain cumulated activity concentration (*25*). Patient-specific splenic cumulated activity concentration was determined using the

actual spleen volume measured from CT images (*26*). The masses of palpable and nonpalpable tumors were determined using calipers and CT or MRI images, respectively. Tumors <2 g by caliper measurement, or <10 g by CT measurement, were excluded from the analysis to ensure accuracy. Lumbar vertebrae marrow imaging was used to calculate the cumulated activity in the marrow (*27*). The uptake of ^{111}In in 3 lumbar vertebrae was extrapolated to uptake in total marrow, assuming that the red marrow mass in the 3 lumbar vertebrae constituted 6.7% of total red marrow mass (*28*).

TIs

To calculate ^{90}Y radiation dosimetry, pharmacokinetic data for ^{90}Y-2IT-BAD-Lym-1 were assumed to be the same as those for ^{111}In-2IT-BAD-Lym-1 (*29*). The AUC for each tissue was converted to radiation dose using MIRD formulas as reported in detail (*13*). TIs were calculated by dividing the radiation dose to the tumor by the radiation dose to each of the normal tissues. In the case of radionuclide therapy, TIs reflect relative tumor and normal tissue effect, albeit lacking radiobiologic factors, such as tissue radiosensitivity.

Chelate Stability and Formation of Metabolites In Vitro

Previously, ^{88}Y-2IT-BAD-Lym-1 showed no measurable decomposition in human serum under physiologic conditions for 25 d (*1*). For this study, the stability of ^{114m}In-2IT-BAD-Lym-1 in human serum was evaluated by similar methods; ^{88}Y and ^{114m}In were used as long-lived analogs of ^{90}Y and ^{111}In to allow prolonged studies. Briefly, ^{114m}In-2IT-BAD-Lym-1 was prepared using methods for ^{111}In-2IT-BAD-Lym-1 radiolabeling as above. ^{114m}In-2IT-BAD-Lym-1 was added to human serum from a volunteer such that the concentrations of ^{114m}In, DOTA, and Lym-1 were 1.9 MBq/mL, 2 μmol/L, and 0.5 μmol/L, respectively. Duplicate solutions were incubated at 37°C in a humidified, 5% carbon dioxide/95% air atmosphere, and a pH of 7.4 ± 0.1 was maintained. Aliquots (10 μL) were removed at 0, 0.83, 1.8, 4.7, 7.1, and 13.8 d and evaluated by native polyacrylamide gel electrophoresis and radioanalytic imaging, as described (*1*), to determine the fraction of ^{114m}In transchelated to serum proteins. Control solutions of ^{114m}In-2IT-BAD-Lym-1 in water and free ^{114m}In in serum were also electrophoresed at every time point to calibrate the migration of all ^{114m}In-labeled species.

To investigate possible mechanisms for the metabolism of ^{111}In-2IT-BAD-Lym-1, as observed in clinical studies, ^{111}In-2IT-BAD-Lym-1 was added to plasma from 2 NHL patients and a volunteer and monitored for formation of metabolites and complexes in vitro. Blood was collected in Vacutainer test tubes coated with buffered sodium citrate. The blood was centrifuged, and plasma was decanted and filtered (0.45 μm). ^{111}In-2IT-BAD-Lym-1 was added to each plasma sample such that the final concentrations of ^{111}In, DOTA, and Lym-1 were 0.37 MBq/mL, 0.023 μmol/L, and 0.017 μmol/L, respectively. The solutions were incubated at 37°C in a humidified, 5% carbon dioxide/95% air atmosphere. Aliquots (100 μL) were removed at 0, 1, 2, 3, and 7 d and evaluated by molecular sieving HPLC to determine the fraction of ^{111}In-2IT-BAD-Lym-1 in the forms of monomer, metabolites, and complexes.

To investigate the role of lymphoma cells in the metabolism of ^{111}In-2IT-BAD-Lym-1, the radiopharmaceutical was added to Raji cell culture and monitored for the formation of metabolites and complexes in vitro. Raji is an American Type Culture Collection–certified cell line, established in 1963 from a Burkitt's lymphoma of the left maxilla of an 11-y-old boy. Three assay cultures were prepared as follows. ^{111}In-2IT-BAD-Lym-1 (15 kBq/110 ng) was added to Raji cells (3×10^6) in medium (0.5 mL) of 10% fetal calf serum/RPMI medium 1640 (GIBCO BRL, Grand Island, NY). The cultures were incubated for 2 h at 37°C in a humidified, 5% carbon dioxide/95% air atmosphere, washed 3 times in medium, and resuspended in medium (0.5 mL). The wash eluants and assay cultures were counted to determine the fraction of ^{111}In-2IT-BAD-Lym-1 bound to the Raji cells. The assay cultures were incubated at 37°C in a humidified, 5% carbon dioxide/95% air atmosphere. At 4 h, 1 assay culture was centrifuged and washed, and the cell pellet and supernatant were counted to determine the fraction of ^{111}In-2IT-BAD-Lym-1 bound to Raji cells. The supernatant was evaluated by HPLC to determine the fraction of ^{111}In-2IT-BAD-Lym-1 in the forms of monomer, metabolites, and complexes. The remaining assay cultures were evaluated similarly at 1 and 2 d. A similar study was performed with a smaller amount of ^{111}In-2IT-BAD-Lym-1 (3.7 kBq/27 ng). Similar studies were performed with ^{125}I-Lym-1 (15 kBq/400 ng and 3.7 kBq/100 ng). Control studies were performed as described, except Raji cells were excluded. Cultures of Raji cells (3×10^6) in medium (0.5 mL) were assessed for viability by exclusion of trypan blue (Sigma) at all time points.

RESULTS

Radiopharmaceuticals

Patient doses of ^{111}In-2IT-BAD-Lym-1, ^{90}Y-2IT-BAD-Lym-1, and ^{111}In-2IT-BAD-m170 showed high structural and functional integrity before injection (Table 1). Similar results were obtained for RICs prepared for in vitro experiments.

TABLE 1
Radiopharmaceutical Quality Assurance Results

Radiopharmaceutical	No. of patients	Radiochemical purity (HPLC)	Monomeric fraction (CAE)	Relative immunoreactivity (RIA)
^{111}In-2IT-BAD-Lym-1	19	100% ± 1.8%	99% ± 4.5%	96% ± 9.3%
^{90}Y-2IT-BAD-Lym-1	3	97% ± 4.4%	98% ± 1.2%	94% ± 5.6%
^{111}In-2IT-BAD-m170	22	99% ± 1.9%	100% ± 0.2%	74% ± 19%

RIA = radioimmunoassay.
Data are presented as mean ± 1 SD.

Metabolites and Complexes

HPLC of ^{111}In-2IT-BAD-Lym-1 radiopharmaceuticals before injection indicated a single peak corresponding to monomeric mAb, but after injection HPLC of patient plasma indicated substantial fractions of metabolites and complexes, which increased over time (Fig. 1). Metabolites and complexes of ^{111}In-2IT-BAD-Lym-1 were observed in the plasma of 18 of 19 NHL patients within 1 d of injection and 19 of 19 patients within 3 d. Three days after injection of ^{111}In-2IT-BAD-Lym-1, a mean ± 1 SD of 1.3 ± 1.4 %ID of ^{111}In was in the patients' blood, after correction for decay, of which monomer, metabolites, and complexes constituted 54% ± 20%, 36% ± 18%, and 10% ± 5.9%, respectively. The extent of metabolism of ^{111}In-2IT-BAD-Lym-1 was not related to splenomegaly, circulating lymphoma cells, histologic marrow lymphoma, or amount of Lym-1 injected.

The apparent metabolism of ^{111}In-2IT-BAD-Lym-1 in NHL patients occurred earlier and to a much greater extent than that of ^{111}In-2IT-BAD-m170 in breast and prostate cancer patients (Fig. 2). Three days after injection of ^{111}In-2IT-BAD-m170 in patients with breast cancer, a mean of 29.2 ± 5.4 %ID of ^{111}In was in the patients' blood, after correction for decay, of which monomer constituted 91% ± 8.8%. The corresponding values for prostate cancer patients were 26.4 ± 3.6 %ID at 3 d, of which 94% ± 12% was monomer. In 12 of 22 breast and prostate cancer patients, no metabolites or complexes of ^{111}In-2IT-BAD-m170 were observed 3 d after injection.

A comparison of ^{111}In-2IT-BAD-Lym-1 and ^{90}Y-2IT-BAD-Lym-1 in the 3 evaluable patients who received both showed that, in individual patients, the formation of ^{111}In and ^{90}Y metabolites and complexes occurred at similar rates (Fig. 3). The immunoprecipitation studies indicated that transchelation of ^{111}In or ^{90}Y from 2IT-BAD-Lym-1 to albumin or transferrin did not occur.

Pharmacokinetics and TIs

In patients receiving ^{111}In-2IT-BAD-Lym-1, the mean values of ^{111}In in the blood were 6.0 ± 7.0, 1.8 ± 2.0, 1.3 ± 1.4, and 0.26 ± 0.14 %ID at 1, 2, 3, and 7 d after injection, respectively. ^{111}In cleared the blood with a β-phase intercept and β-phase half-time of 16% ± 20% and 1.5 ± 1.7 d, respectively. The mean blood AUC was 0.83 kBq · h/g/MBq injected. The contribution of ^{111}In-2IT-BAD-Lym-1 monomer to the total blood AUC was calculated. ^{111}In-2IT-BAD-Lym-1 monomer cleared the blood with a β-phase intercept and β-phase half-time of 16% ± 20% and 1.0 ± 0.7 d, respectively. The mean blood AUC from ^{111}In-2IT-BAD-Lym-1 monomer was 0.75 kBq · h/g/MBq. Thus, because monomeric ^{111}In-2IT-BAD-Lym-1 was the predominant species in blood at early time points and contributed 90% of the AUC (0.75/0.83), the pharmacokinetic parameters of all ^{111}In in the blood and monomeric ^{111}In-2IT-BAD-Lym-1 in the blood were similar. However, ^{111}In in the blood associated with nonmonomeric species grew over time and provided 10% of total blood AUC, a substantial fraction.

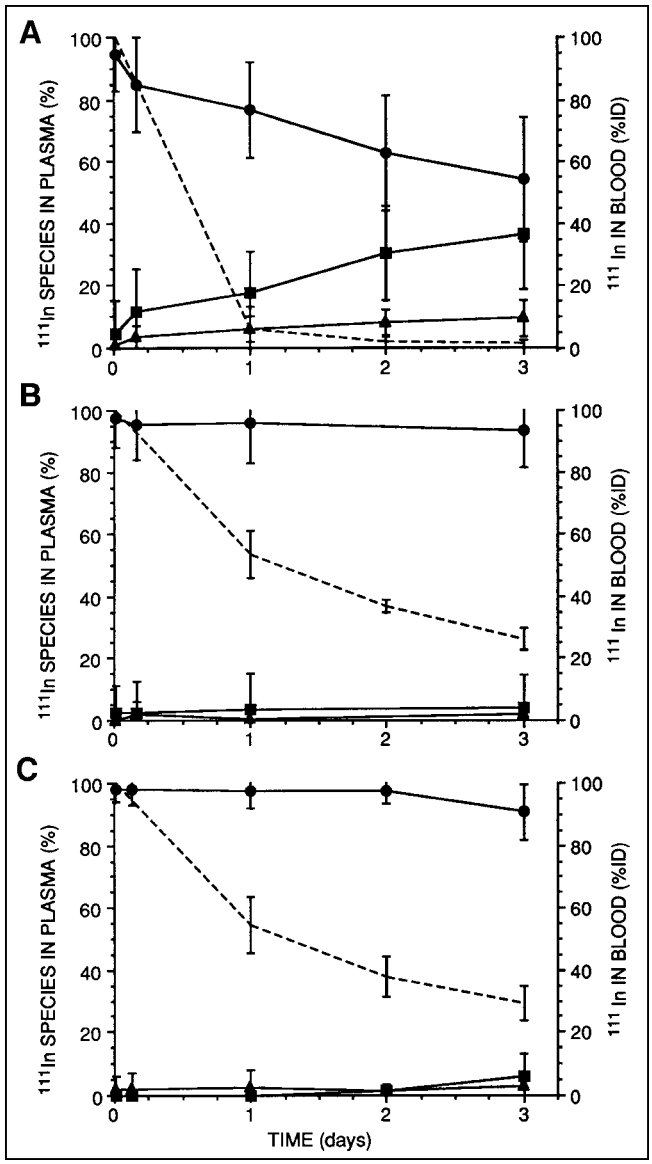

FIGURE 2. Comparison of metabolism of ^{111}In-2IT-BAD-Lym-1 in NHL patients (A), ^{111}In-2IT-BAD-m170 in prostate cancer patients (B), and ^{111}In-2IT-BAD-m170 in breast cancer patients (C). Of ^{111}In-2IT-BAD-Lym-1 or ^{111}In-2IT-BAD-m170 in patients' plasma at specific points in time, percentage in monomeric (●), metabolite (■), and complexed (▲) forms was measured by HPLC. In NHL patients receiving ^{111}In-2IT-BAD-Lym-1, metabolites and complexes constituted substantially larger fractions of ^{111}In in plasma compared with prostate and breast cancer patients receiving ^{111}In-2IT-BAD-m170. Decay-corrected mean percentage injected dose (%ID) of ^{111}In in patients' blood decreased over time (dashed lines). Thus, metabolites and complexes of ^{111}In-2IT-BAD-Lym-1 showed relative growth over time as fractions of total ^{111}In activity, but not absolute growth in terms of %ID.

For every patient who received ^{111}In/^{90}Y-2IT-BAD-Lym-1, the AUC for tumor was greater than the AUC for marrow, kidneys, and lungs. However, in many patients, the AUC for liver or spleen was greater than that for tumor (Table 2). TIs for ^{90}Y-2IT-BAD-Lym-1 were tumor/total

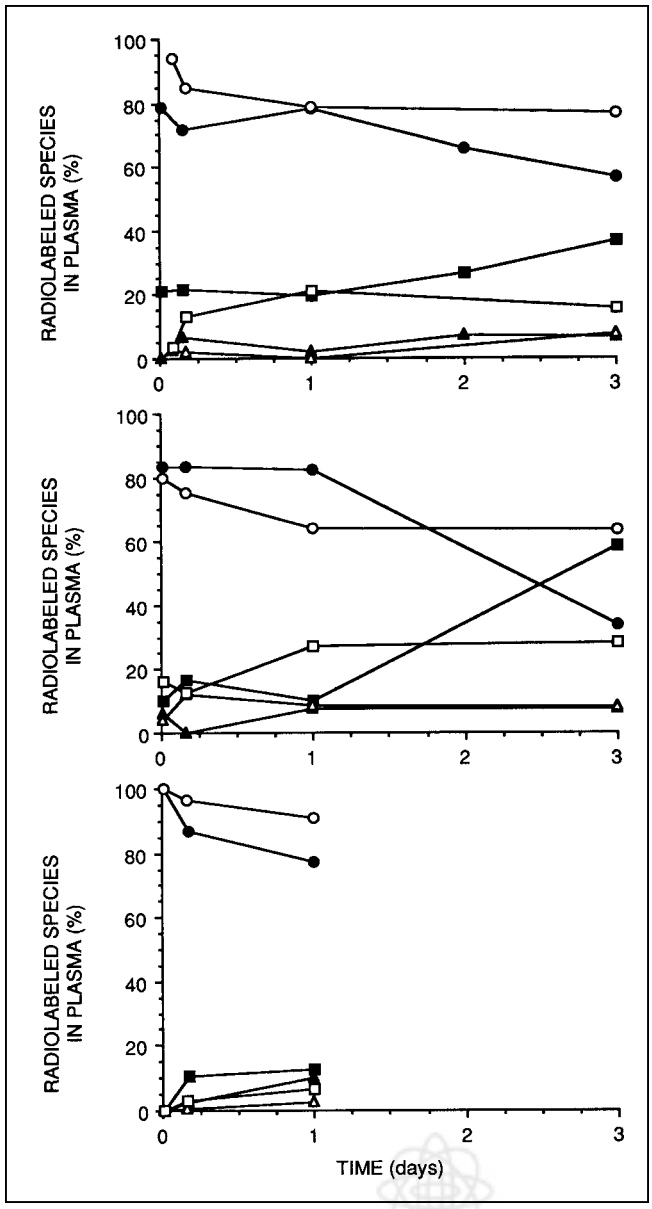

FIGURE 3. Comparison of formation of metabolites and complexes of ^{111}In-2IT-BAD-Lym-1 and ^{90}Y-2IT-BAD-Lym-1. Each graph represents 1 NHL patient who received ^{111}In- and ^{90}Y-2IT-BAD-Lym-1 in close temporal proximity. Of ^{111}In-2IT-BAD-Lym-1 in patients' plasma at specific points in time, percentage in monomeric (●), metabolite (■), and complexed (▲) forms was measured by HPLC. Of ^{90}Y-2IT-BAD-Lym-1 in patients' plasma at specific points in time, percentage in monomeric (○), metabolite (□), and complexed (△) forms was measured by HPLC. Extent of formation of nonmonomeric forms of ^{111}In- and ^{90}Y-2IT-BAD-Lym-1 was similar in individual patients.

body, 13.6; tumor/marrow, 3.7 (lumbar imaging method); tumor/liver, 1.2; tumor/lungs, 5.3; tumor/kidneys, 2.5; and tumor/blood, 15.7.

The mean cumulative excretion of ^{111}In in urine was 4.5 ± 2.2, 12.7 ± 4.7, and 21.2 ± 6.8 %ID of ^{111}In-2IT-BAD-Lym-1 at 1, 2, and 3 d, respectively.

In Vitro Studies

Polyacrylamide gel electrophoresis of ^{114m}In-2IT-BAD-Lym-1 in serum from a volunteer showed that 98.0%, 98.1%, 98.4%, 97.5%, 97.3%, 96.9%, and 96.5% of ^{114m}In was associated with 2IT-BAD-Lym-1 at 0, 0.83, 1.8, 4.7, 7.1, 10.2, and 13.8 d, respectively, indicating a loss of ^{114m}In at a rate of 0.13% per day by transfer to serum proteins or cleavage from Lym-1 antibody.

^{111}In-2IT-BAD-Lym-1 added to the plasma of 2 NHL patients in vitro formed metabolites and complexes similar to those of the volunteer and much less than in vivo (Table 3). At 3 d, 92.6%, 89.1%, and 85.8% of ^{111}In was associated with monomer in the plasma of the 2 NHL patients and the volunteer, respectively, in the in vitro study. Comparatively, at 3 d, a mean of only 54.0% of ^{111}In was associated with monomer in the plasma of all patients in vivo.

^{111}In-2IT-BAD-Lym-1 in Raji cell culture was examined. The Raji cells were at least 94% viable up to 48 h. The following data pertain to the Raji cell cultures containing 15 kBq ^{111}In-2IT-BAD-Lym-1, but similar results were obtained in the 3.7-kBq studies. Most ^{111}In remained associated with the Raji cells, 79% at 48 h (Table 4). The remainder of the ^{111}In, dissociated from the Raji cells and in the supernatant, was in the forms of monomer, 14.8%; metabolite, 5.1%; and complex, 1.1%. ^{125}I-Lym-1 showed greater formation of metabolites, and the ^{125}I-Lym-1 metabolites were smaller in size (data not shown).

DISCUSSION

Metabolites of iodinated antibodies and, less frequently, radiometal-labeled antibodies have been reported in patient urine but, to our knowledge, not in patient plasma; therefore, the observation of radiolabeled metabolites of ^{111}In/^{90}Y-2IT-BAD-Lym-1 in patient plasma was unexpected. It is not apparent whether the absence of reports of metabolites in the plasma of patients receiving ^{111}In- or ^{90}Y-labeled antibodies reflects the fact that metabolites are uncommonly formed or that diagnostic assays are uncommonly performed or reported. In earlier studies, metabolites of ^{131}I-Lym-1 or ^{67}Cu-2IT-BAT-Lym-1 were generally not observed in patient plasma using HPLC, although it is possible that they were formed and then rapidly excreted.

The fraction of radiolabeled metabolites of ^{111}In-2IT-BAD-Lym-1 in plasma grew to 36% at 3 d, and ^{90}Y data were similar. The fraction of total radiopharmaceutical that had undergone metabolism up to that time was likely different because plasma represents a single compartment in a dynamic system: Nearly 99% of the injected dose of ^{111}In had cleared the blood in 3 d, species entered and left the plasma and related interstitial space, and the pharmacokinetics of metabolites and whole antibody were likely different. Regardless, on the basis of frequent sampling and analysis of patient plasma, nonmonomeric species contributed a mean 10% of cumulated activity in the blood (kBq·h/mL plasma per MBq injected). The nonmonomeric fraction was less likely to be immunoreactive or capable of

TABLE 2
AUC of ^{111}In (kBq·h/g of Tissue per MBq Injected) from ^{111}In-2IT-BAD-Lym-1

Patient no.	Total body	Blood*			Liver	Spleen	Kidneys	Lungs	Marrow (L3)†	Tumors
		From monomer	From nonmonomeric species	Total						
1	1.04	1.29	0.30	1.59	8.19	11.40	6.11	3.35	4.05	10.27
2	1.00	0.15	0.05	0.20	13.97	9.20	7.18	2.67	1.40	7.65
3	1.01	0.56	0.06	0.62	8.44	19.40	5.03	2.64	5.19	5.39
4	0.90	1.06	0.07	1.13	9.10	16.10	4.78	2.79	0.62	10.58
5	0.98	0.11	0.01	0.12	11.96	28.70	6.90	2.31	0.03	20.45
6	0.94	0.18	0.20	0.38	6.81	10.39	2.46	2.17	3.45	25.77
7	0.95	0.22	0.04	0.26	11.61	17.28	6.90	2.56	1.47	10.20
8	0.98	0.77	0.01	0.78	10.78	29.72	6.67	2.80	2.82	‡
9	1.19	0.51	0.01	0.52	15.43	44.50	4.95	2.72	2.49	7.88
10	0.88	0.80	0.02	0.82	14.74	21.25	3.99	2.49	2.36	10.26
11	0.92	2.27	0.06	2.33	11.91	30.23	5.39	2.41	2.67	11.17
12	0.92	0.86	0.19	1.05	13.82	42.12	4.53	2.47	6.57	‡
13	0.94	0.15	0.13	0.28	11.31	§	3.85	2.66	3.13	8.14
14	0.97	0.23	0.01	0.24	15.23	25.10	7.59	1.90	2.58	6.07
15	0.92	1.29	0.04	1.33	8.00	37.82	5.95	1.58	2.62	17.64
16	0.95	1.99	0.18	2.17	8.36	35.21	4.13	2.51	3.33	17.71
17	0.99	0.98	0.13	1.11	7.92	29.76	4.17	3.40	11.47	23.11
18	0.91	0.19	0.07	0.26	15.08	§	8.14	2.83	5.06	19.00
19	0.98	0.70	0.00	0.70	7.29	14.43	3.50	1.06	7.25	‡
Mean	0.97	0.75	0.08	0.84	11.05	24.86	5.38	2.49	3.61	13.21
± SD	± 0.07	± 0.61	± 0.08	± 0.63	± 2.92	± 10.77	± 1.52	± 0.53	± 2.58	± 6.21

*AUC from monomer + AUC from nonmonomeric species (complexes and metabolites) = total blood AUC.
†Lumbar imaging.
§Splenectomy.
‡Tumor(s) too small for accurate volume measurement.

active tumor uptake, resulting in lower TIs for ^{111}In/^{90}Y-2IT-BAD-Lym-1. TIs for the total body, marrow, liver, kidneys, spleen, and blood for ^{111}In/^{90}Y-2IT-BAD-Lym-1 were lower than those reported for ^{67}Cu-2IT-BAT-Lym-1 (*30*), suggesting that metabolism of ^{111}In/^{90}Y-2IT-BAD-Lym-1 had an adverse effect on the TI.

The metabolism of ^{111}In/^{90}Y-2IT-BAD-Lym-1 may affect its uptake and retention in tumors and normal tissues. Complexes may or may not retain immunoreactivity but are likely to be extracted by the phagocytic cells of the reticuloendothelial system of the liver, spleen, bone marrow, and elsewhere. Metabolites are often readily excreted through the kidneys or, less commonly, the gastrointestinal (GI) tract but may be trapped (dependent on the nature and size of the metabolites) by the renal tubular cells or other tissues, particularly when the metabolites are radiometal labeled (Fig. 4). Generally, ^{111}In was readily visualized in the GI tract of the NHL patients who received ^{111}In-2IT-BAD-

TABLE 3
^{111}In-2IT-BAD-Lym-1 in Plasma of 1 Volunteer and 2 NHL Patients In Vitro: % Monomer/% Metabolites/% Complexes

Time (d)	Volunteer	NHL patient	NHL patient
0*	100/0.0/0.0	100/0.0/0.0	100/0.0/0.0
0†	89.4/3.2/7.4	93.9/4.9/1.2	90.0/4.4/5.6
1	87.5/3.1/9.4	93.8/3.6/2.5	86.8/6.7/6.5
2	87.9/3.6/8.5	93.0/5.1/1.9	89.5/4.4/6.1
3	85.8/4.4/9.8	92.6/5.1/2.3	89.1/4.4/6.5
7	No data	92.3/4.7/3.0	85.3/4.6/10.1

*Before addition to plasma.
†After addition to plasma.

TABLE 4
Processing of ^{111}In-2IT-BAD-Lym-1 and ^{125}I-Lym-1 in Raji Cell Culture

Time (d)	% cell bound/% released intact/% released metabolites/% released complexes	
	^{111}In-2IT-BAD-Lym-1*	^{125}I-Lym-1*
0.17	84/12.2/1.8/2.0	91/6.5/2.0/0.5
1	82/14.4/3.2/0.5	85/10.7/3.5/0.8
2	79/14.8/5.1/1.1	80/7.9/10.9/1.2

*100% of ^{111}In and ^{125}I was on intact Lym-1 before addition to Raji cells.

Lym-1 but not the breast and prostate cancer patients who received ^{111}In-2IT-BAD-m170 (Fig. 5).

The data support processing of ^{111}In/^{90}Y-2IT-BAD-Lym-1 in the hepatocytes as the dominant mechanism for the production of metabolites. Antibody processing with metabolite induction usually occurs in the hepatocytes; specific hepatocyte receptors have been documented for mouse IgG2a antibodies, such as Lym-1 (*31*,*32*), but not for mouse IgG1 antibodies, such as m170, consistent with the presence of ^{111}In-2IT-BAD-Lym-1 metabolites and the absence of ^{111}In-2IT-BAD-m170 metabolites in patient plasma. Hepatocyte processing is supported by the imaging evidence for ^{111}In in the GI tract of patients given Lym-1 (Fig. 5). The observation of a significant metabolite fraction in plasma soon after injection (Fig. 2A) indicates the involvement of a well-perfused system in the formation of metabolites. All NHL patients received an amount of unlabeled Lym-1 that was documented in earlier studies to be sufficient to saturate the Lym-1 receptor on hepatocytes (*31*). It is conceivable that the hepatocytes were able to discriminate the ^{111}In- or ^{90}Y-2IT-BAD-Lym-1 from the unlabeled Lym-1, thereby permitting uptake and metabolism. However, processing by hepatocytes does not explain the ^{111}In/^{90}Y-2IT-BAD-Lym-1 complexes in the plasma, which accounted for about one fourth of the nonmonomeric species. Because of the practical and conceptual importance of definition of the mechanism for formation of the metabolites, hepatocyte involvement should be investigated further—specifically, the effect of chemical modification of antibody for interaction with hepatocyte molecules.

Other possible mechanisms of formation of the nonmonomeric radiolabeled ^{111}In and ^{90}Y species in the plasma were considered, evaluated against clinical data, and, in some cases, investigated further in vitro, specifically: instability of the ^{111}In and ^{90}Y RICs; complexation by antigen or HAMA in the plasma and extraction with metabolism by phagocytic cells; and uptake, internalization, and metabolism by lymphoma cells or normal B-lymphocytes.

The exceptional stability of the chelate moiety and the conjugate linker of In- and Y-2IT-BAD-Lym-1 in human serum under physiologic conditions in vitro has been shown here and elsewhere (*1*). The stability of ^{111}In- and ^{90}Y-2IT-BAD-m170 in the plasma of patients with breast or prostrate cancer in vivo also corroborated the stability of the chelate

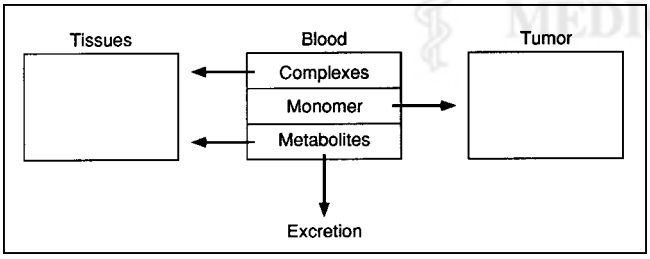

FIGURE 4. Simplified model for distribution of ^{111}In/^{90}Y-2IT-BAD-Lym-1 RIC in circulation in blood. Monomeric RIC is preferentially distributed to tumor, whereas metabolites and complexes of RIC are excreted or distributed to normal tissues. Thus, formation of metabolites and complexes of ^{111}In/^{90}Y-2IT-BAD-Lym-1 resulted in reduced cumulated activity in tumor and increased cumulated activity in normal tissues (lower TIs and higher toxicity).

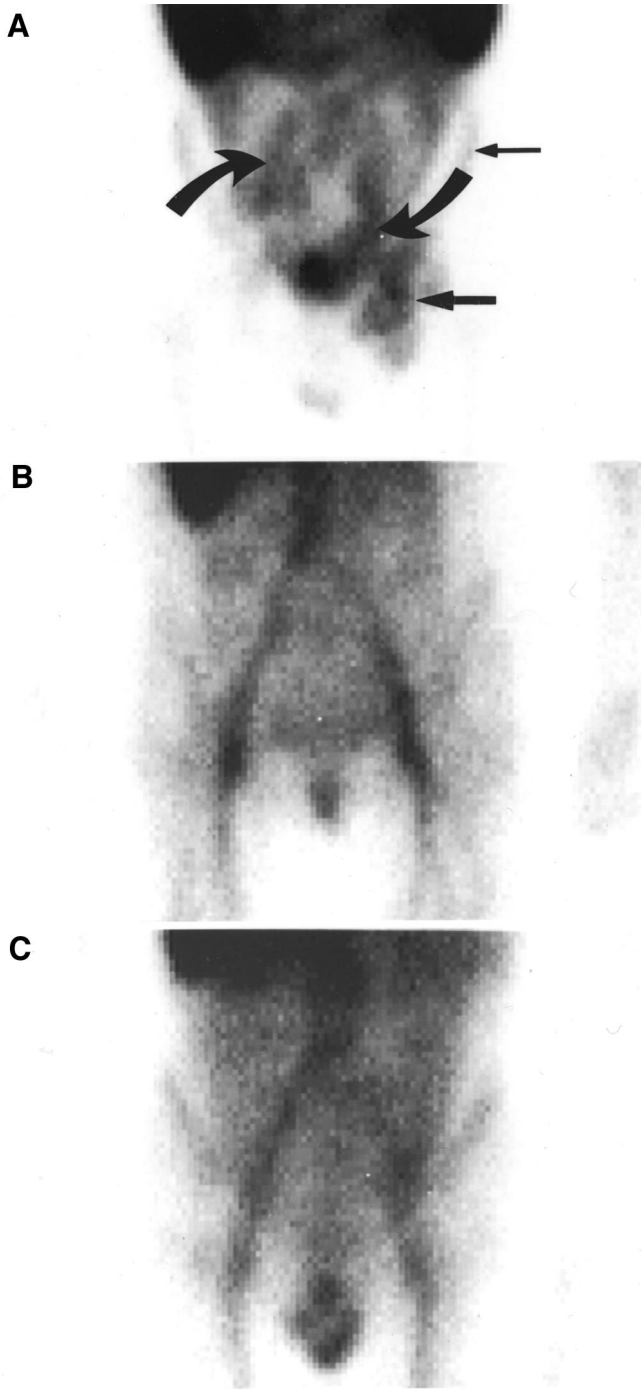

FIGURE 5. Planar anterior view of pelvis of NHL patient given ^{111}In-2IT-BAD-Lym-1 (A) and breast (B) and prostate (C) cancer patients given ^{111}In-2IT-BAD-m170, 3 d after injection. In addition to ^{111}In in lymphoma (↤) and marrow (←), ^{111}In was present in GI tract (↩) of patient with NHL but not in patients with breast and prostate cancer. Specific hepatocyte receptors have been documented for mouse IgG2a antibodies, such as Lym-1, but not for mouse IgG1 antibodies, such as m170.

and conjugate linker. Finally, immunoprecipitation studies of plasma of patients who had received ^{111}In- and ^{90}Y-2IT-BAD-Lym-1 indicated that transchelation of ^{111}In or ^{90}Y from 2IT-BAD-Lym-1 to albumin or transferrin did not occur in vivo. In evaluating specifically for the metabolism of ^{111}In-2IT-BAD-Lym-1 in vitro, metabolites and complexes were formed to a minor extent in lymphoma plasma in vitro, similar to volunteer plasma (Table 3), and the in vitro results were quantitatively insufficient to explain the in vivo events observed in the NHL patients. Because all NHL patients tested negative for HAMA, complexation and phagocytosis with subsequent metabolism were also unlikely.

Lastly, the possible uptake and metabolism of ^{111}In/^{90}Y-2IT-BAD-Lym-1 by normal or malignant NHL lymphocytes (or both) were considered. Two patients who exhibited substantial metabolite fractions in plasma, despite lacking a pool of normal B-lymphocytes, provide anecdotal evidence against normal lymphocytes. One patient had no spleen and the second patient had B-lymphocyte depletion associated with earlier rituximab (Rituxan; IDEC Pharmaceuticals Corp., San Diego, CA) therapy. Furthermore, the HLA-DR antigen is low in density on the surface membrane of normal B-lymphocytes and has not been observed to be a source of significant Lym-1 binding (*33*). In the case of malignant NHL lymphocytes, the degree of internalization of Lym-1 in Raji human Burkitt's lymphoma cells or NHL cells has been variously reported as low (*34*) to quite high, followed by rapid metabolism and excretion (*35*). However, in the latter report, ^{111}In-radiolabeled Lym-1 was residualized in Raji cells. Our study indicated that, at 48 h, only 5% of ^{111}In-DOTA-2IT-BAD-Lym-1 was released as metabolites by Raji cells in vitro and did not support substantial lymphocyte involvement in the metabolite formation observed in patients. Most but not all NHL patients had large tumor burdens, but no relationship between tumor burden and metabolite formation was found. A few patients had quite small tumor burdens yet had substantial metabolite formation.

The observation of metabolites of ^{111}In/^{90}Y-2IT-BAD-Lym-1 in patient plasma, but not of ^{131}I-Lym-1 or ^{67}Cu-2IT-BAD-Lym-1, indicates the remarkable influence of the radiolabel on the cellular processing of radiolabeled antibodies. It is well documented that degraded radiometal-labeled antibodies residualize in cells, but iodinated antibodies are degraded to small species (i.e., iodotyrosine) that are rapidly excreted. It has been shown that ^{67}Cu-ceruloplasmin is a major degradation or transcomplexation product of ^{67}Cu-2IT-BAT-Lym-1. With a MW of 150 kDa, ^{67}Cu-ceruloplasmin in patient plasma was indistinguishable from ^{67}Cu-2IT-BAD-Lym-1 by HPLC but was identified by immunoprecipitation studies (*16*).

Cellular processing of iodinated and radiometal-labeled mAbs has been investigated in cell culture and animal models (*4–6,32,35–39*); similar studies of ^{111}In/^{90}Y-2IT-BAD-Lym-1, though beyond the scope of this investigation, may be instructive. Although these observations have potential importance for all RICs and emphasize the need to document the nature of the radiolabeled species in the plasma (and urine and stool), they may not necessarily be extrapolated to other RICs. The discrepant results for the other radiolabeled mAb, ^{111}In- and ^{90}Y-2IT-BAD-m170, are probably more representative of the common circumstance. Juweid et al. (*40*) have shown substantial improvement in TIs for ^{111}In- or ^{90}Y-labeled humanized LL2 anti-CD22 mAb compared with ^{131}I-labeled mAb in NHL patients, although results for HPLC or immunoreactivity were not reported.

CONCLUSION

Molecular sieving HPLC indicated the presence of metabolites and complexes in the plasma of every NHL patient soon after injection of ^{111}In- and ^{90}Y-2IT-BAD-Lym-1, despite the stability of these RICs in vitro. Metabolism of ^{90}Y-2IT-BAD-Lym-1 in the NHL patients appeared to reduce TIs for radiation dose. Clinical data and subsequent in vitro studies suggested processing of ^{111}In/^{90}Y-2IT-BAD-Lym-1 in the hepatocytes as the dominant mechanism for the production of metabolites.

ACKNOWLEDGMENTS

This research was supported by National Cancer Institute grants PO1 CA47829 and CA16861, Berlex Research Agreement 94K058, and Department of Energy grant DE FG03-84ER60233.

REFERENCES

1. Deshpande SV, DeNardo SJ, Kukis DL, et al. Yttrium-90-labeled monoclonal antibody for therapy: labeling by a new macrocyclic bifunctional chelating agent. *J Nucl Med*. 1990;31:473–479.
2. Kukis DL, Diril H, Greiner DP, et al. A comparative study of copper-67 radiolabeling and kinetic stabilities of antibody-macrocycle chelate conjugates. *Cancer*. 1994;73(suppl):779–786.
3. DeNardo GL, DeNardo SJ, Miyao NP, et al. Non-dehalogenation mechanisms for excretion of radioiodine after administration of labeled antibodies. *Int J Biol Markers*. 1988;3:1–9.
4. Shih LB, Thorpe SR, Griffiths GL, et al. The processing and fate of antibodies and their radiolabels bound to the surface of tumor cells in vitro: a comparison of nine radiolabels. *J Nucl Med*. 1994;35:899–908.
5. Press OW, Shan D, Howell-Clark J, et al. Comparative metabolism and retention of iodine-125, yttrium-90, and indium-111 radioimmunoconjugates by cancer cells. *Cancer Res*. 1996;56:2123–2129.
6. Hanna R, Ong GL, Mattes MJ. Processing of antibodies bound to B-cell lymphomas and other hematological malignancies. *Cancer Res*. 1996;56:3062–3068.
7. Hu E, Epstein AL, Naeve GS, et al. A phase 1a clinical trial of Lym-1 monoclonal antibody serotherapy in patients with refractory B cell malignancies. *Hematol Oncol*. 1989;7:155–166.
8. DeNardo GL, DeNardo SJ, Shen S, et al. Factors affecting ^{131}I-Lym-1 pharmacokinetics and radiation dosimetry in patients with non-Hodgkin's lymphoma and chronic lymphocytic leukemia. *J Nucl Med*. 1999;40:1317–1326.
9. DeNardo GL, Lamborn KR, Goldstein DS, Kroger LA, DeNardo SJ. Increased survival associated with radiolabeled Lym-1 therapy for non-Hodgkin's lymphoma (NHL) and chronic lymphocytic leukemia (CLL). *Cancer*. 1997; 80(suppl):2706–2711.
10. DeNardo GL, DeNardo SJ, Goldstein DS, et al. Maximum tolerated dose, toxicity, and efficacy of ^{131}I-Lym-1 antibody for fractionated radioimmunotherapy of non-Hodgkin's lymphoma. *J Clin Oncol*. 1998;16:3246–3256.
11. O'Donnell RT, DeNardo GL, Kukis DL, et al. ^{67}Copper-2-iminothiolane-6-[p-

(bromoacetamido)benzyl-TETA-Lym-1 for radioimmunotherapy of non-Hodgkin's lymphoma. *Clin Cancer Res*. 1999;10:3330–3336.
12. Wessels BW, Rogus RD. Radionuclide selection and model adsorbed dose calculations for radiolabeled tumor associated antibodies. *Med Phys*. 1984;11: 638–645.
13. DeNardo GL, O'Donnell RT, Shen S, et al. Radiation dosimetry for ^{90}Y-2IT-BAD-Lym-1 extrapolated from pharmacokinetics using ^{111}In-2IT-BAD-Lym-1 in patients with non-Hodgkin's lymphoma. *J Nucl Med*. 2000;41:952–958.
14. Kukis DL, DeNardo SJ, DeNardo GL, O'Donnell RT, Meares CF. Optimized conditions for chelation of yttrium-90-DOTA immunoconjugates. *J Nucl Med*. 1998;39:2105–2110.
15. DeNardo SJ, Richman CM, Goldstein DS, et al. Yttrium-90/indium-111-DOTA-peptide-chimeric L6: pharmacokinetics, dosimetry and initial results in patients with incurable breast cancer. *Anticancer Res*. 1997;17:1735–1744.
16. Mirick GR, O'Donnell RT, DeNardo SJ, Shen S, Meares CF, DeNardo GL. Transfer of copper from a chelated ^{67}Cu-antibody conjugate to ceruloplasmin in lymphoma patients. *Nucl Med Biol*. 1999;26:841–845.
17. Wong JY, Williams LE, Yamauchi DM, et al. Initial experience evaluating ^{90}yttrium-radiolabeled anti-carcinoembryonic antigen chimeric T84.66 in a phase I radioimmunotherapy trial. *Cancer Res*. 1995;55:5929–5934.
18. National Cancer Institute sponsored study of classifications of non-Hodgkin's lymphomas: summary and description of a working formulation for clinical usage: The Non-Hodgkin's Lymphoma Pathologic Classification Project. *Cancer*. 1982;49:2112–2135.
19. Rose LM, Gunasekera AH, DeNardo SJ, DeNardo GL, Meares CF. Lymphoma-selective antibody Lym-1 recognizes a discontinuous epitope on the light chain of HLA-DR10. *Cancer Immunol Immunother*. 1996;43:26–30.
20. Richman CM, DeNardo SJ, O'Donnell RT, et al. Dosimetry-based therapy in metastatic breast cancer patients using ^{90}Y monoclonal antibodies 170H.82 with autologous stem cell support and cyclosporin A. *Clin Cancer Res*. 1999;5(10 suppl):3243S–3248S.
21. Howell LP, DeNardo SJ, Levy N, Lund J, DeNardo GL. Immunohistochemical staining of metastatic ductal carcinomas of the breast by monoclonal antibodies used in imaging and therapy: a comparative study. *Int J Biol Markers*. 1995;10: 126–135.
22. Kukis DL, DeNardo GL, DeNardo SJ, et al. Effect of the extent of chelate substitution on the immunoreactivity and biodistribution of 2IT-BAT-Lym-1 immunoconjugates. *Cancer Res*. 1995;55:878–884.
23. DeNardo GL, DeNardo SJ, O'Grady LF, Levy NB, Adams GP, Mills SL. Fractionated radioimmunotherapy of B-cell malignancies with ^{131}I- Lym-1. *Cancer Res*. 1990;50(suppl):1014–1016.
24. Erwin WD, Groch MW, Macey DJ, DeNardo GL, DeNardo SJ, Shen S. A radioimmunoimaging and MIRD dosimetry treatment planning program for radioimmunotherapy. *Nucl Med Biol*. 1996;23:525–532.
25. Snyder WS, Ford MR, Warner GG. "*S*" *Absorbed Dose per Unit Cumulated Activity for Selected Radionuclides and Organs. MIRD Pamphlet No. 11*. New York, NY: Society of Nuclear Medicine; 1975:82–83.
26. Shen S, DeNardo GL, O'Donnell RT, Yuan A, DeNardo DA, DeNardo SJ. Impact of splenomegaly on therapeutic response and I-131-LYM-1 dosimetry in patients with B-lymphocytic malignancies. *Cancer*. 1997;80(suppl):2553–2558.
27. Lim S-M, DeNardo GL, DeNardo DA, et al. Prediction of myelotoxicity using radiation doses to marrow from body, blood and marrow sources. *J Nucl Med*. 1997;38:1374–1378.
28. Brodsky A. *CRC Handbook of Radiation Measurements and Protection, Section A Volume II: Biological and Mathematical Information*. Boca Raton, FL: CRC Press; 1982:148–150.
29. Carrasquillo JA, White JD, Paik CH, et al. Similarities and differences in ^{111}In- and ^{90}Y-labeled 1B4M-DTPA antiTac monoclonal antibody distribution. *J Nucl Med*. 1999;40:268–276.
30. DeNardo GL, Kukis DL, Shen S, DeNardo DA, Meares CF, DeNardo SJ. Copper-67 versus iodine-131 labeled Lym-1 antibody: comparative pharmacokinetics and dosimetry in patients with non-Hodgkin's lymphoma. *Clin Cancer Res*. 1999;5:533–541.
31. Adams GP, DeNardo SJ, Deshpande SV, et al. Effect of mass of ^{111}In-benzyl-EDTA monoclonal antibody on hepatic uptake and processing in mice. *Cancer Res*. 1989;49:1707–1711.
32. Junghans RP, Anderson CL. The protection receptor for IgG catabolism is the β_2-microglobulin-containing neonatal intestinal transport receptor. *Proc Natl Acad Sci USA*. 1996;93:5512–5516.
33. Rose LM, Deng CT, Scott S, et al. Critical Lym-1 binding residues on polymorphic HLA-DR molecules. *Mol Immunol*. 1999;36:789–797.
34. Epstein AL, Marder RJ, Winter JN, et al. Two new monoclonal antibodies, Lym-1 and Lym-2, reactive with human-B-lymphocytes and derived tumors, with immunodiagnostic and immunotherapeutic potential. *Cancer Res*. 1987;47:830–840.
35. Ong GL, Mattes MJ. Processing of antibodies to the MHC class II antigen by B-cell lymphomas: release of Fab-like fragments into the medium. *Mol Immunol*. 1999;36:777–788.
36. Geissler F, Anderson SK, Venkatesan P, Press OW. Intracellular catabolism of radiolabeled anti-μ antibodies by malignant B cells. *Cancer Res*. 1992;52:2907–2915.
37. Novak-Hofer I, Zimmermann K, Maecke HR, Amstutz HP, Carrel F, Schubiger PA. Tumor uptake and metabolism of copper-67-labeled monoclonal antibody chCE7 in nude mice bearing neuroblastoma xenografts. *J Nucl Med*. 1997;38: 536–544.
38. Stein R, Goldenberg DM, Thorpe SR, Mattes MJ. Advantage of a residualizing iodine radiolabel for radioimmunotherapy of xenografts of human non-small-cell carcinoma of the lung. *J Nucl Med*. 1997;38:391–395.
39. Rogers BE, Anderson CJ, Connett JM, et al. Comparison of four bifunctional chelates for radiolabeling monoclonal antibodies with copper radioisotopes: biodistribution and metabolism. *Bioconjugate Chem*. 1996;7:511–522.
40. Juweid ME, Stadtmauer E, Sharkey RM, et al. Pharmacokinetics, dosimetry and initial therapeutic results with ^{131}I- and ^{111}In-/^{90}Y-labeled humanized LL2 anti-CD22 monoclonal antibody (MAb) in patients with relapsed/refractory non-Hodgkin's lymphoma (NHL). *Clin Cancer Res*. 1999;5(10 suppl):3292S–3303S.